

Original Article

Evaluation of locomotor function and microscopic structure of the spinal cord in a mouse model of experimental autoimmune encephalomyelitis following treatment with syngeneic mesenchymal stem cells

Nilesh Kumar Mitra¹, Umesh Bindal¹, Wong Eng Hwa¹, Caroline LL Chua², Chek Ying Tan³

¹School of Medicine, Taylor's University, Lakeside Campus, Subang Jaya, Selangor, Malaysia; ²School of Biosciences, Taylor's University, Lakeside Campus, Subang Jaya, Selangor, Malaysia; ³Research Laboratory, School of Medicine, Pharmacy and Biosciences, Taylor's University, Lakeside Campus, Subang Jaya, Selangor, Malaysia

Received August 7, 2015; Accepted September 21, 2015; Epub October 1, 2015; Published October 15, 2015

Abstract: Out of the minor myelin proteins, most significant one is myelin oligodendrocyte glycoprotein (MOG). Mesenchymal stem cells (MSCs) have proven immunoregulatory capacity. The objective of this study was to investigate the effects of syngeneic MSCs on mouse model of experimental autoimmune encephalomyelitis (EAE) through observation of locomotion by footprint analysis, histological analysis of spinal cord and estimation IL-17. C57BL/6 mice (10 weeks, n = 16) were immunized with 300 µg of MOG₃₅₋₅₅ and 200 µL of complete Freund's adjuvant (CFA) to produce EAE model. Sham-treated control (n = 8) were injected with CFA. Half of immunized mice were given 100 µL of PBS (n = 8) and next half (n = 8) received 1×10^5 MSCs on day 11 through the tail veins. Clinical scoring showed development of EAE (loss of tonicity of tail and weakness of hind limb) on day 10. Following MSC treatment, clinical scores and hindlimb stride length showed significant improvement on day 15 onwards, compared to day 10 (P < 0.05). Under LFB staining, while PBS-treated group of EAE mice showed pale and degenerated axons in anterolateral white column of lumbar spinal cord, MSC-treated group showed numerous normal-looking axons. H&E staining showed normal axons in anterolateral white column and reduction of macrophages in MSC-treated EAE mice group. A lower level of IL-17 was observed in MSC treated EAE mice, compared to PBS-treated EAE mice. Our results suggest that Intravenous MSC has the potential to improve the locomotion and regeneration of axons in spinal cord in MOG-induced EAE model.

Keywords: Experimental autoimmune encephalomyelitis, mesenchymal stem cells, footprint analysis, histology, spinal cord

Introduction

Out of the various autoimmune demyelinating diseases affecting the central nervous system, incidence of multiple sclerosis (MS), a chronic demyelinating disease has been reported to be higher [1]. Perivascular infiltration of immune cells across the blood-brain barrier was observed as one of the pathological characteristics of MS [2]. Various types of immune cells including T cells, B cells, activated macrophages and microglia have been found to be involved in the inflammation and demyelination associated with MS in histopathological studies [3]. In particular, T-lymphocytes have been implicated in the autoimmune responses

against myelin antigens, as shown in the animal model of experimental autoimmune encephalomyelitis (EAE) [4]. Many of the therapeutic modalities related to the clinical studies of MS was evolved out of the mechanisms observed in the studies involving regulation of EAE in inbred rat and mice model [5]. MOG myelin protein has been found in the outermost turn of the myelin membrane. MOG has been proposed to play a role in transducing signals through the membrane of the myelin to the cytoskeleton elements during myelin sheath formation by oligodendrocyte [6]. A previous study has reported that peripheral blood lymphocytes from MS patients responded predominantly to MOG compared to myelin basic protein (MBP), sug-

gesting its importance in the pathogenesis of MS [7].

EAE can be induced, as a chronic disease, in C57BL/6 mouse by immunization with MOG [8] and it manifests morphological changes of demyelination, inflammation and axonal loss, similar to human MS [9]. Mesenchymal stem cells (MSC) are multipotent cells capable of differentiating into different cell types such as osteocytes, adipocytes and chondrocytes [10]. MSCs are capable of repairing tissue injuries by creating a milieu that promotes the regeneration of endogenous cells [11]. An anti-apoptotic mechanism activated by the MSCs was proposed to influence the regeneration process and affect the functional outcome after stem cell treatment in neurodegenerative diseases [12]. The immunoregulatory capacity of the MSCs to suppress T-cell responses was demonstrated both in vitro and in vivo [13, 14]. In this study, an animal model of EAE was produced in C57BL/6 mouse by immunization with MOG. MSCs were isolated from the primary culture of bone-chips that were isolated from young and healthy C57BL/6 mouse and were characterized by flow cytometry. The effects of intravenous administration of MSCs from syngeneic young mice to the EAE mouse of C57BL/6 strain were investigated by using histological analysis, measurement of IL-17 levels and estimation of locomotion by footprint analysis.

Materials and methods

Animals and induction of EAE

Female C57BL/6 mice (8-10 weeks old) were procured from and maintained in the animal holding facility of Brain Research Institute of Monash University Sunway Campus Malaysia. MOG peptide, corresponding to 21 mouse MOG amino acid residues, was synthesized by ProspecBio (Israel). On day 0 (zero), mice (n = 16) received subcutaneous injections of 300 µg of the MOG₃₅₋₅₅ peptide mixed with 200 µL of complete Freund's adjuvant (CFA) containing 4 mg/ml heat-killed H37Ra strain of *Mycobacterium tuberculosis* (Chondrex Inc.) over the tail pleat followed by intra-peritoneal administration of 400 ng of pertussis toxin (PT) (Sigma-Aldrich). The second post-immunization dose of PT was also administered IP on day 2. The mice were examined and scored daily for clinical

signs of EAE using a protocol adapted from the University of Pennsylvania's Institutional Animal Care and Use Committee guideline (IACUC guideline experimental autoimmune encephalomyelitis rodent models). The standard clinical score criteria used were as follows: 0 = no signs, 1 = limp tail, 2 = limp tail and mild paralysis of hind limbs, 3 = paralysis of hind limbs or with urinary incontinence, 4 = hind limb paralysis with weakness of forelimbs or with atonic bladder and 5 = quadriplegia. The animal protocol was approved by the animal ethics committee of the Monash University. Sham-treated EAE mice (n = 8), that were injected with CFA followed by PT were used as controls.

Isolation and proliferation of MSCs

C57BL/6 mice (n = 6) were sacrificed under anesthesia followed by cervical dislocation. Femur, tibia and humerus bones were cut in between the upper and lower epiphyses and were collected under aseptic conditions. Bone marrow was flushed out by injecting Hank's balanced salt solution into the medullary cavity, until the bone pieces became pale. The bone pieces were digested in a mixture of Dulbecco's Modified Eagle Medium (DMEM) and Collagenase II (GIBCO). Following the formation of a coagulum in a shaking incubator, the bone chips were washed multiple times and plated in a 25-cm² plastic culture flask in low glucose DMEM supplemented with fetal bovine serum (FBS) and antibiotics. The culture flasks were kept in a humidified 5% CO₂ incubator at 37°C. On the third day, the non-adherent circular floating cells were removed by a complete media change. After seven days, the adherent MSCs were harvested by trypsinisation with 0.25% trypsin containing 1 mM EDTA. Cell count was done using the Trypan blue exclusion assay and plating was done at variable densities ranging from 1600 to 2500 cells/cm². The adherent MSCs were cultured in consecutive passages once per week at a split ratio of 1:2 until the fifth passage.

Characterization of MSCs

The MSCs obtained in passage-4 culture were plated in Mesencult proliferation media followed by basal media containing 20% Mesencult adipogenic stimulatory supplement (Stemcell Technologies, Canada). After three weeks, differentiated adipocytes were fixed

Effect of MSC on EAE model in mouse

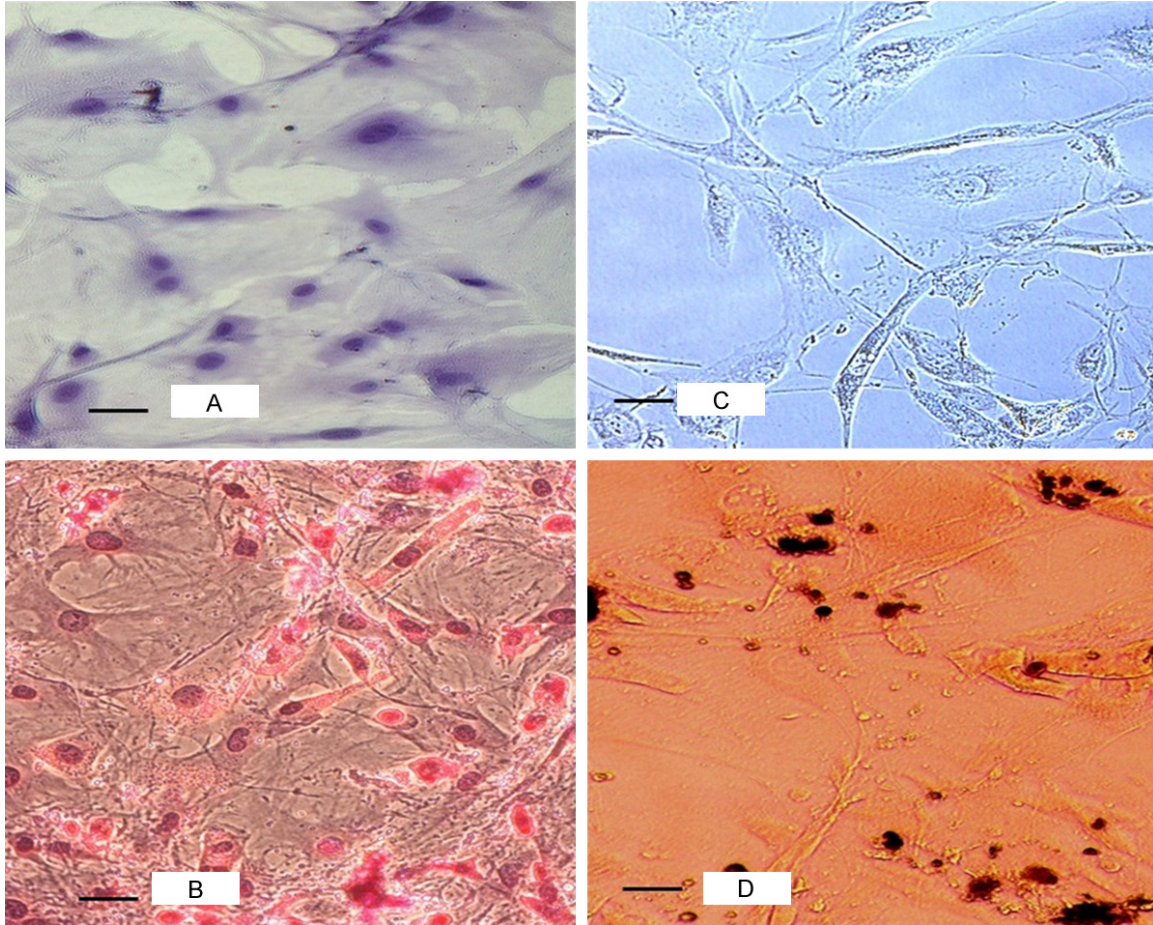


Figure 1. Phase contrast photomicroscopy of multilineage differentiation of MSCs derived from C57BL/6 mouse bone-chips culture. Control undifferentiated MSCs (A) and fat droplets in differentiated adipocytes stained red (B) (20 \times , Oil Red O stain). Control undifferentiated MSCs (C) and dark brown calcium salt deposits in the extracellular matrix of differentiated osteoblast cells (D) (20 \times , von Kossa stain).

with 4% paraformaldehyde (PFA) and stained with oil red O (**Figure 1A** and **1B**). Similarly, osteogenic differentiation was done in Mesencult basal media containing 25% Mesencult osteogenic stimulatory supplement (Stemcell Technologies, Canada). After three weeks, the appearance of calcium salts at the bottom of the plate was identified using von Kossa stain after fixation with 4% PFA and incubation with 1% silver nitrate for two hours (**Figure 1C** and **1D**). MSCs were analyzed for cell surface marker expression at passage-4 and passage-5. The cells were trypsinised, washed with staining buffer and incubated (1×10^5 cells in 100 μ L) with combination of antibodies (10 μ L each) for 45 minutes in the dark at room temperature. The antibodies used were CFS-anti-rat-CD105, PE-anti-rat-CD29, APC-anti-rat-Sca-1 and PerCP-anti-rat-CD45 (R&D

Systems, USA). Samples were run using the BD Accuri™ C6 flow cytometer and results were analyzed using CFlow Plus software. Isotype-matched antibodies were used as controls to determine non-specific staining. Flow cytometry analysis revealed that more than 98% of the MSCs expressed Sca-1 and more than 63% of the MSCs expressed CD29 (**Figure 2**). A small percentage (9.8%) of the cultured cells was positive for CD105. Absence of CD45 positive cells (0.6%) indicated that the culture was devoid of cells of hematopoietic origin. Minimum expression of CD-105 antigen in these compact-bone derived MSCs can be attributed with promising experimental study value [15] as it was proposed that CD105-negative cells suppressed the proliferation of CD4⁺ T cells more efficiently compared to CD105 positive cells [16].

Effect of MSC on EAE model in mouse

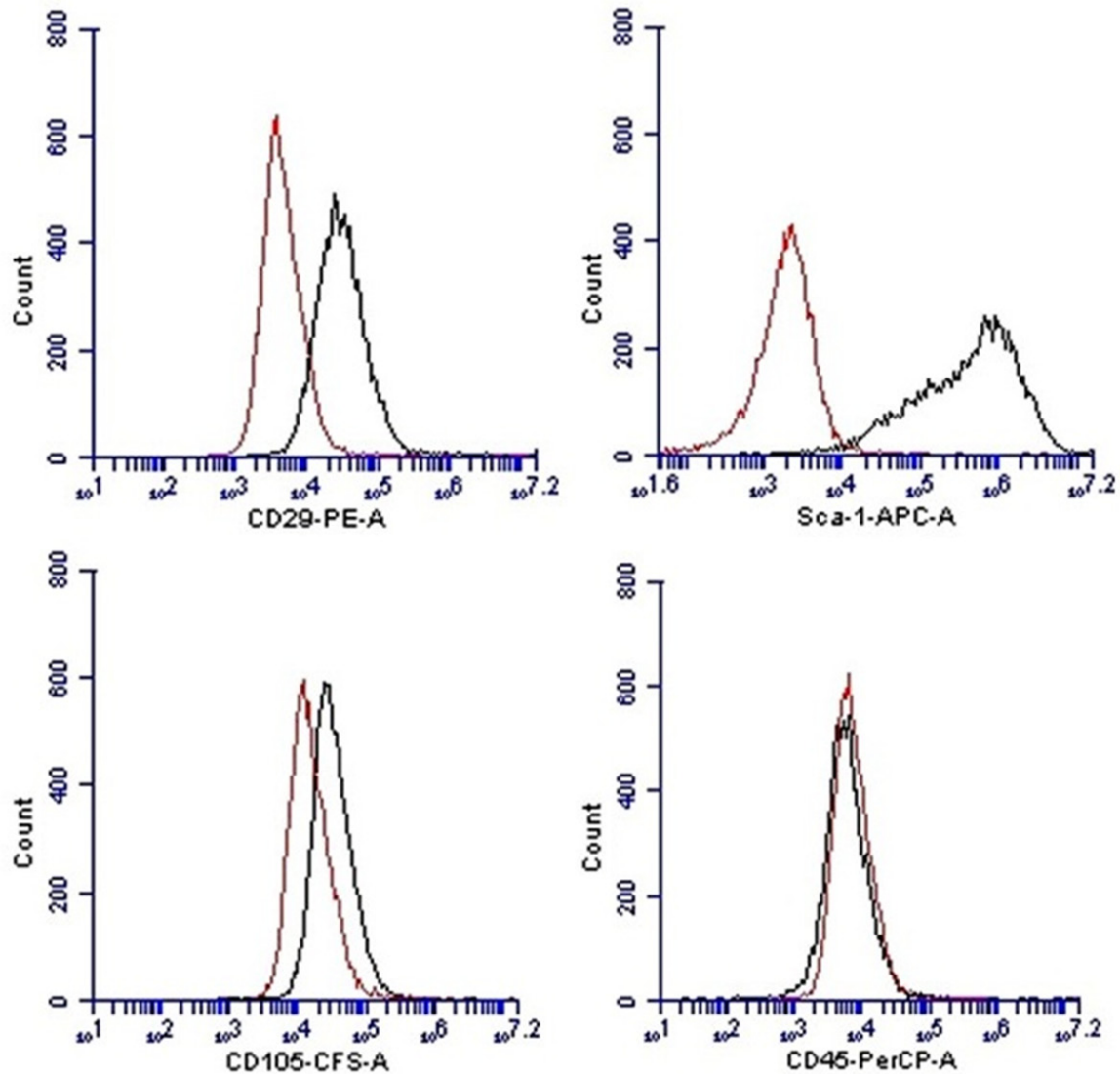


Figure 2. Flow cytometry analysis for phenotypic characterization of compact bone derived MSCs. The histogram with red line shows isotype controls and histogram with gray lines show reactivity with indicated antibodies. Majority of cells were positive for Sca-1 (98.2%) and CD-29 (63.4%). Only a small subpopulation of cells (9.8%) was positive for CD-105. Cultured MSCs showed lack of CD-45 expression.

Injection of MSCs

The mice that had developed EAE (by 10th day) (n = 16) were divided into two groups, as follows: Group 1, control group, received 100 μ L of PBS by intravenous route (n = 8) and Group 2, MSC treated group, received 1×10^5 MSCs by intravenous route (n = 8). The injections of MSC or PBS through the tail veins were done on day 11 of MOG immunization, with the mice being kept in an immobilizer. Mean daily scores, pre-treatment scores (day 0 to day 10), and post-treatment scores (day 11 to day 20) were calculated for each group.

Footprint analysis

The footprint analysis done on day 0 (pre-experiment), day 5, day 10, day 15 and day 20 were used to compare the gait of PBS treated EAE mice with that of MSC treated EAE mice. The forepaws and hindpaws of the mouse were stained with red and blue organic colours by dipping over the stamp-pad. The mouse was then allowed to run through a 50-cm-long and 10-cm-wide paper-lined plastic tunnel to a goal-box, creating consecutive footprints of forelimb and hindlimb with red and blue colours. At least nine steps were measured for each mouse.

Effect of MSC on EAE model in mouse

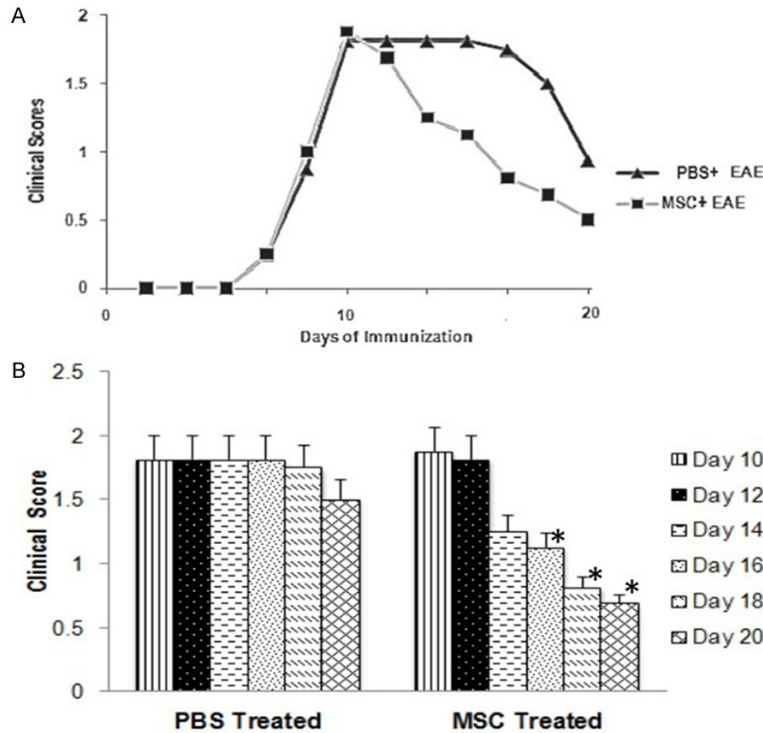


Figure 3. Mean clinical score observed in PBS treated EAE mice group and MSC treated EAE mice group from day 0 to day 20 (A). Comparison between the scores in PBS treated and MSC treated group (mean \pm S.E.) (B). Significant reduction in the scores day 16 onwards (* $P < 0.05$) in MSC treated group compared to day 10 score in one way repeated measures ANOVA.

Three steps from the middle portion of each run were measured for the data on stride and stance lengths. Three readings were taken with a gap of 30 minutes each to prevent stress to the mouse. A fresh sheet of white paper was placed on the floor of the runway for each run. A piece of wet paper towel was placed at the opposite end of the tunnel, to wipe the ink on the paws. Measurements of stride length, fore-base width, and hind-base width gave an indication of gait. Stride length was measured for forelimb and hindlimb as the average distance of forward movement between each stride. The mean values for each set of three values of stride length, fore-base width and hind-base width were used in subsequent analysis. Statistical analysis of one way repeated measures ANOVA was carried out to determine any significant difference ($P < 0.05$) between the values of footprint analysis on day 0, day 5, day 10, day 15 and day 20.

Histological analysis

Four mice in each group were transcardially perfused with normal saline through the left

cardiac ventricle followed by fixation with cold 4% PFA on 22nd day of the MOG immunisation. Spinal cords were carefully dissected out, post-fixed in 4% PFA for 24 hours, and processed for paraffin embedding. Sections were cut at 8 μ m on a Leica semi-automatic microtome and stained for histologic examination under an Olympus Provis AX70 optical microscope. Hematoxylin and eosin (H&E) staining was used to reveal perivascular or sub-pial inflammatory infiltrates, and Luxol Fast Blue (LFB) staining, was used for the screening of any demyelination.

IL-17 quantification

Splenic tissues from all three groups ($n = 8$ each) were weighed and homogenized with calcium and magnesium-free PBS by gentleMACS dissociator. Splenic supernatant with a concentration of 0.1 mg/ μ L homogenate/protein was stored at -80°C until use. IL-17 cytokine was assayed in supernatants from the splenic homogenate using Quantikine[®] mouse IL-17 immunoassay (R&D Systems Inc. USA) ELISA kit. For each splenic sample, 2 sets of reactions were set up. The 96-well microplate was precoated with a monoclonal antibody specific for mouse IL-17. After 50 μ L of assay diluent was added to each well, 50 μ L of control, standard and sample (splenic homogenate) were added into each well. Following incubation for 2 hours at room temperature, each well was washed for five times with wash buffer. Mouse IL-17 conjugate was added to each well followed by incubation for 2 hours and repeated washing. Following addition of 100 μ L of substrate solution and incubation for 30 minutes in dark, 100 μ L stop solution was added to stop this reaction. The plate was read at 450 nm-540 nm using a microplate reader. A standard curve was constructed from a set of standards with known concentration and this was then used to determine the concentration of IL-17 for each condition.

Effect of MSC on EAE model in mouse

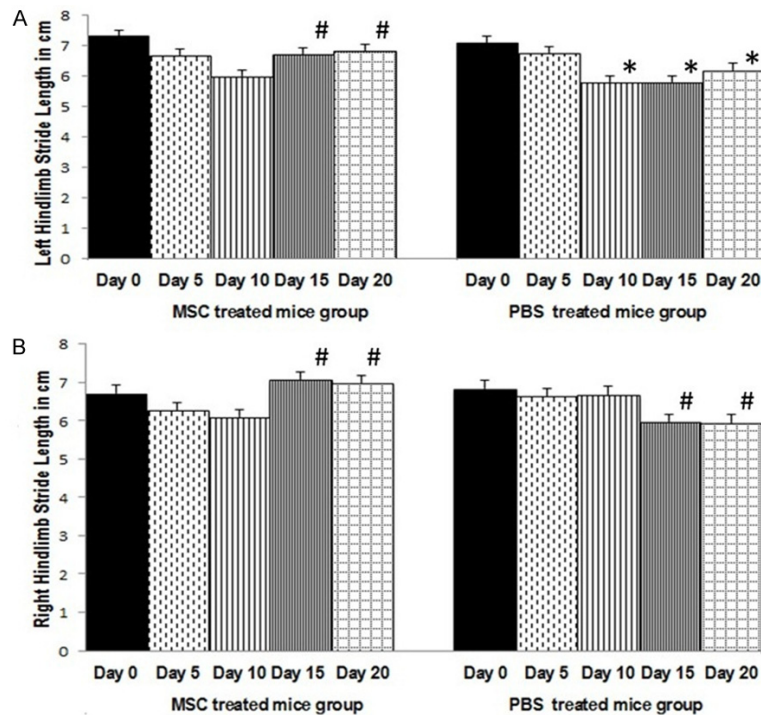


Figure 4. Mean left hindlimb stride length in cm (\pm S.E) (A) and mean right hindlimb stride length in cm (\pm S.E) (B) in PBS treated and MSC treated EAE mice groups. In PBS treated EAE mice group ($n = 8$), significant reduction in hindlimb stride length on day 10 onwards ($*P < 0.05$) (left) and day 15 onwards ($\#P < 0.05$) (right), compared to pre-experiment day 0. In MSC treated EAE mice group ($n = 8$), significant increase in left and right hindlimb stride length on day 15 onwards ($\#P < 0.05$) compared to day 10 stride length. MSC treatment was given on day 11. One way repeated measures ANOVA with post hoc Bonferroni.

Statistical analysis

The results are expressed as mean \pm standard error of mean. The intergroup differences analysis was performed by the two-way ANOVA followed by the post-hoc test of Bonferroni. In the case of nonparametric data analysis, the Mann-Whitney post-hoc test was performed. In all analyses, differences between groups were considered to be significant when $P < 0.05$.

Results

Clinical score evaluation of EAE mouse

The mean clinical score of EAE mice treated with PBS showed appearance of limp tail (score 1) at day 8 with progressive increase in manifestation of symptoms until day 10 when paralysis of hindlimb was observed in addition to limp tail (mean score 1.81) (Figure 3A). After day 16, the mean score decreased gradually

reaching a score of 1 at day 20. Following IV injections of MSC on day 10 (mean score 1.88), MSC-treated EAE mice showed a progressive decrease in the manifestation of symptoms characterized by a continuous decrease in the mean clinical score by 33% on day 14 and 57% on day 18, compared to the mean clinical score on day 10 before administration of MSC. On day 20, the mean clinical score of MSC-treated EAE mice reached a score of 0.5 (Figure 3A). One way repeated measures ANOVA analysis showed significant increase in the mean clinical score on day 16 onwards compared to day 10 in MSC-treated EAE mice (day 16, $P = 0.038$; day 18, $P = 0.008$; day 20, $P = 0.001$). Clinical scores of PBS-treated EAE mice did not show any significant difference between day 10 mean clinical score and mean clinical score on any days afterward (day 12-day 20) (Figure 3B).

Evaluation of foot print analysis in EAE mice

There was no recognisable change in the mean fore-base width and the hind-base width in foot print analysis between any of the three groups of mice. Sham-treated control EAE mice group did not show any significant change in the mean hindlimb stride length in one way repeated measures ANOVA analysis between pre-experiment day 0 data and any of the post-experiment data (day 5, 10, 15, 20). Mean value for left hindlimb stride length in PBS-treated EAE mice group showed significant reduction on day 10, 15, 20 compared to day 0 mean value for pre-experiment stride length [Wilk's lambda = 0.33, $F(4,20) = 9.97$, $P = 0.001$, post-hoc Bonferroni] (Figure 4A). Mean value for right hindlimb stride length in PBS-treated EAE mice group showed significant reduction on day 15 and 20 compared to day 10 mean value for stride length [Wilk's lambda = 0.54, $F(4,20) = 4.23$, $P = 0.012$, post-hoc Bonferroni] (Figure 4B).

Effect of MSC on EAE model in mouse

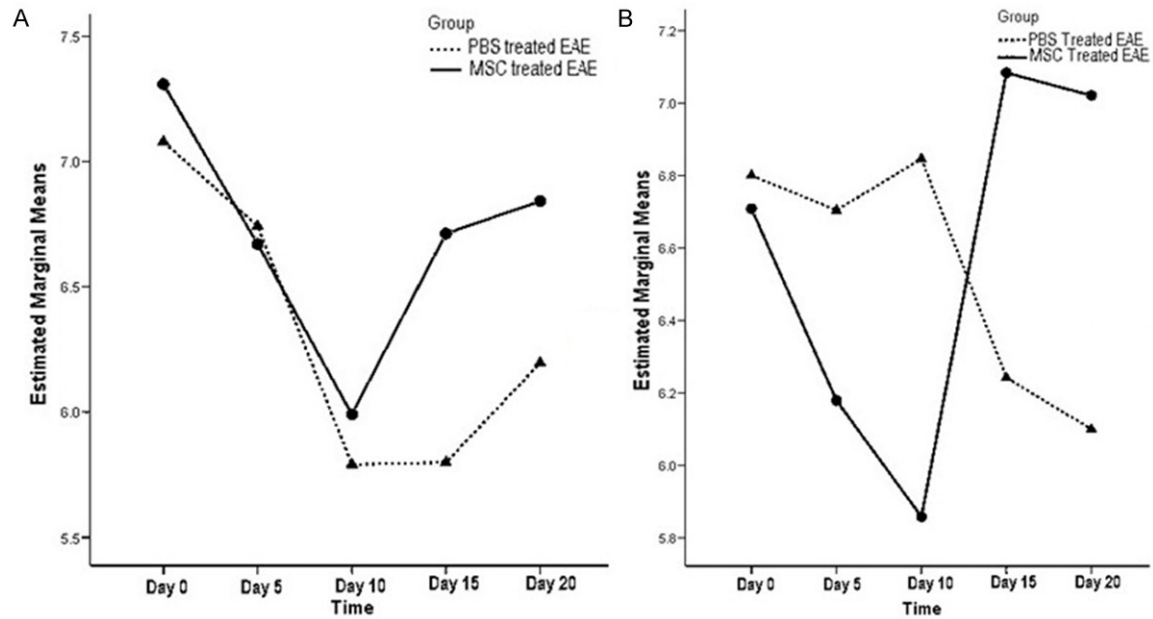


Figure 5. Profile plot of mean left hindlimb stride length (A) and mean right hindlimb stride length (B) in PBS treated and MSC treated EAE mice groups in two way repeated measures ANOVA analysis. Mean stride length on day 15 and day 20 were significantly ($P < 0.05$) higher in MSC treated group.

Evaluation of foot print analysis in EAE mice following MSC treatment

The mean hind limb stride length in EAE mice was compared between MSC-treated group (MSC treatment on day 11) and PBS-treated group. The profile plot in two way repeated measures ANOVA showed significant increase in the mean value for left hindlimb stride length on day 15 and 20, compared to day 10 in MSC-treated EAE mice group (**Figure 5A**). The mean value for left hindlimb stride length on day 20 (6.8 ± 0.9 cm) in MSC-treated EAE mice group was higher than similar mean stride length on day 20 (6.1 ± 0.9 cm) in PBS-treated EAE mice group. Two way repeated measures ANOVA analysis found significant difference in the mean left hind limb stride length between PBS-treated EAE mice group and MSC-treated EAE mice group [Wilk's lambda = 0.63, $F(4,20) = 2.92$, $P = 0.04$]. Significant difference was also observed in the mean value for right hind limb stride length between PBS-treated EAE mice group and MSC-treated EAE mice group [Wilk's lambda = 0.27, $F(4,14) = 9.27$, $P = 0.001$]. In profile plot of two way repeated measures ANOVA (**Figure 5B**), MSC-treated EAE mice group showed significant elevation in the mean value for right hind limb stride length on day 15

(7.1 ± 0.6 cm) and 20 (6.9 ± 0.8 cm), compared to day 10 (6 ± 0.9 cm). In comparison, PBS-treated EAE mice group showed significant reduction in the mean value for right hindlimb stride length on day 15 (5.98 ± 0.7 cm) and day 20 (5.95 ± 0.9) (**Figures 4B and 5B**).

Evaluation of histological analysis

Under LFB staining, compared to the sham-treated control group of mice showing normal bluish-stained myelin (**Figure 6A**), PBS-treated EAE group of mice showed evidence of damage in the myelin sheath of the lateral white funiculus of the lumbar spinal cord sections (**Figure 6B**). The damaged myelin in the lateral white funiculus failed to take the LFB staining in spinal cord sections of PBS-treated EAE mice. In MSC-treated EAE group of mice (**Figure 6C**), normal-looking bluish-stained myelin was observed under LFB staining in the lateral funiculus.

Under H&E staining, sham-treated control group of mice showed rounded axons with a rim of myelin in the white matter of anterior and lateral funiculi of spinal cord sections. The white matter of posterior funiculus also showed normal appearance of axons and uniform endothelial lining around the capillary (**Figure 7A, 7D**).

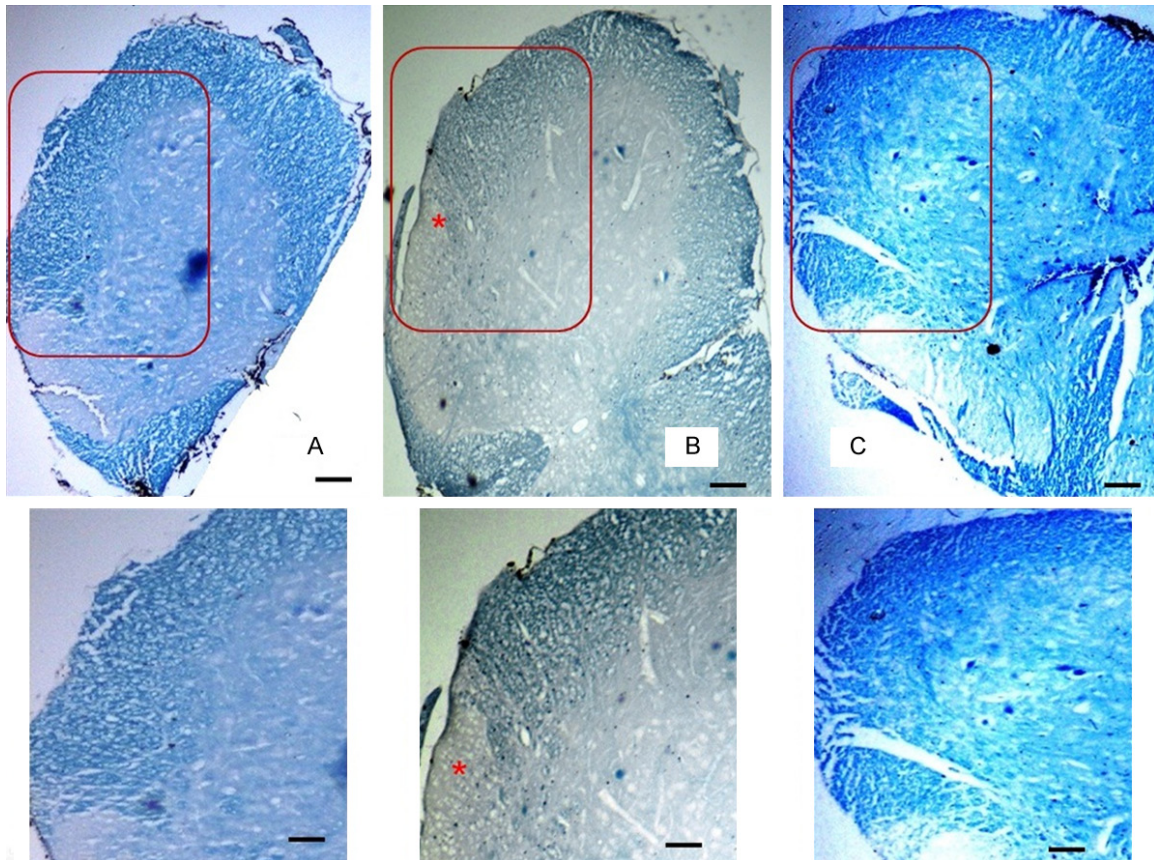


Figure 6. Photomicrograph showing the white matter of anterior and lateral funiculi of the lumbar spinal cord in different groups stained with luxol fast blue (8 μ m, 40 \times , 50 μ m bar). The area of section within the red square has been magnified to show in the box below. Well stained myelin in the white matter in the control sham treated group (A), pale stained myelin in the white matter with an area completely unstained in lateral funiculus (*) in the PBS treated EAE group (B) and well stained myelin in the white matter in MSC treated EAE group (C).

The PBS-treated EAE group of mice showed sub-pial accumulation of macrophages with a loss of normal architecture of the axons in the white matter of anterior and lateral funiculi. Vacuolations were observed at the peripheral part of the funiculi with absence of normal-looking round axons. There was also evidence of neuronal damage with observable pyknosis of nuclei of neurons in the anterior grey column. The white matter of posterior funiculus showed appearance of macrophages in sub-pial region and around the capillaries (**Figure 7B, 7E**). The MSC-treated EAE group of mice showed many normal looking axons surrounded by a rim of myelin in the white matter of anterior and lateral funiculi. The anterior grey column showed neurons with clear nucleus and nucleolus. Although no quantitative analysis was done, there appeared to be fewer macrophages in the sub-pial regions of spinal cord sections in the

MSC-treated EAE group of mice. There was absence of macrophages around the capillary also (**Figure 7C, 7F**).

IL-17 concentration in spleen

Mean concentration of IL-17 from the splenic homogenate estimated by the Quantikine® mouse IL-17 immunoassay on the 22nd day, was increased by 19% in the PBS-treated EAE group of mice, compared to the concentration in sham treated-control group of mice. Splenic homogenate of MSC-treated EAE group of mice showed reduction in the mean IL-17 concentration (**Figure 8**). The mean IL-17 concentration in MSC treated group was reduced by 22%, compared to the mean IL-17 concentration in PBS treated EAE group. The reduction of the mean IL-17 concentration in the MSC treated group of mice was not statistically significant.

Effect of MSC on EAE model in mouse

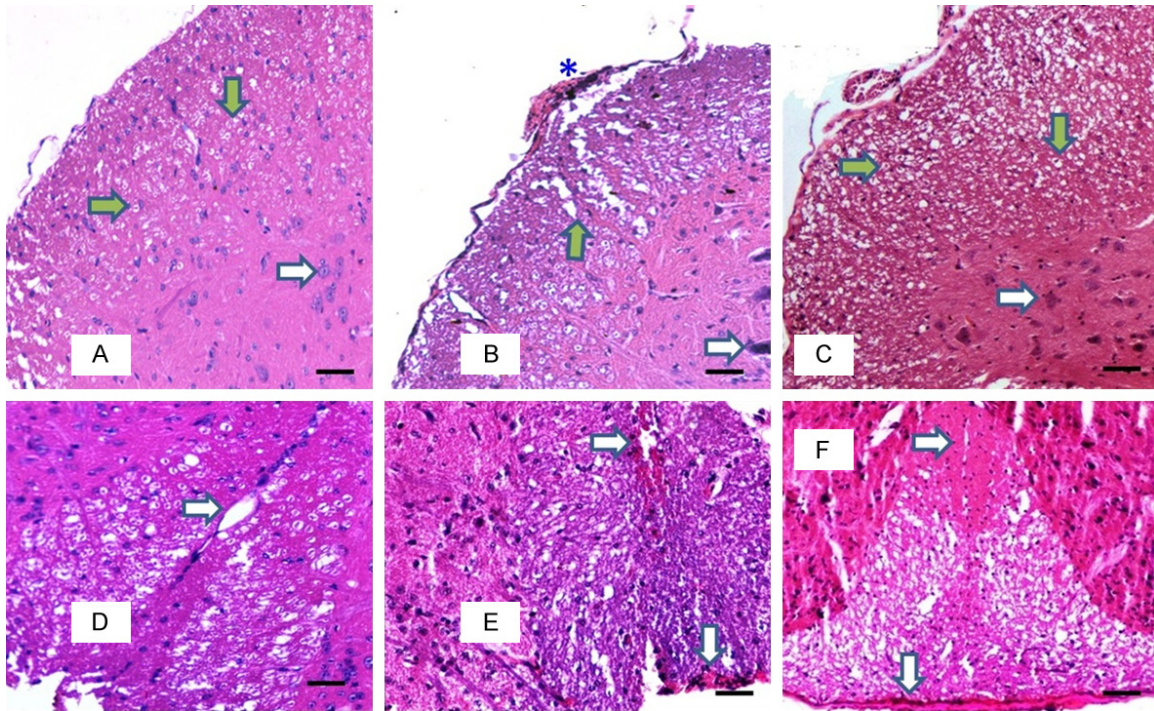


Figure 7. Photomicrograph showing the white matter of anterolateral funiculus (A-C) and posterior funiculus (D-F) of the lumbar spinal cord in different groups stained with H&E (8 μ m, 100 \times , 50 μ m bar). Green arrows showing the dot-shaped axon surrounded by rim of unstained myelin in the white matter and white arrow showing the normal-looking neuron in the anterior grey column in the control sham treated group (A). Normal posterior white funiculus with capillary (white arrow) in control sham treated group (D). Areas of demyelinated white matter with vacuolation (green arrow), pyknotic neuron (white arrow) and macrophages (*) in PBS treated EAE group (B). Macrophages in sub-pial and pericapillary locations are also seen (white arrow) (E). Normal looking white matter with dot-shaped axon surrounded by rim of unstained myelin in MSC treated EAE group (C). Posterior white column showing lack of macrophages (white arrow) in MSC treated group (F).

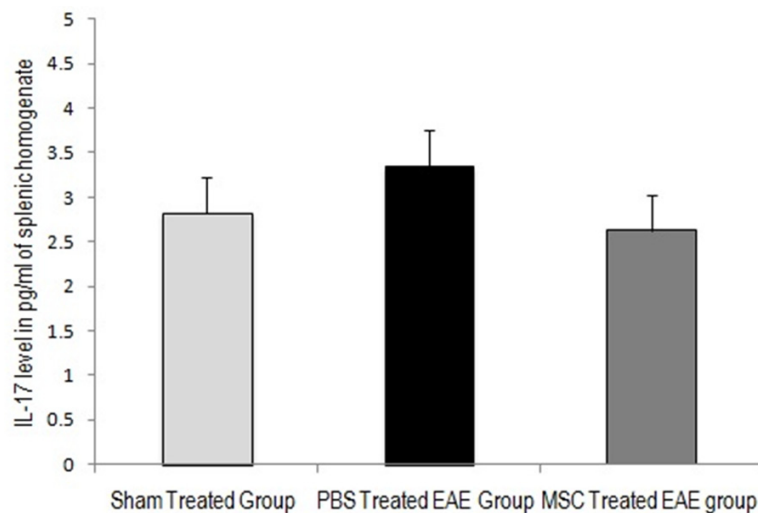


Figure 8. Mean (\pm S.E) concentration of IL-17 in pg/ml of splenic homogenate (collected on 22nd day) in sham treated control group, PBS treated EAE group and MSC treated EAE group. Mean concentration of IL-17 increased with MOG treatment in PBS treated EAE group. Following MSC treatment IL-17 concentration decreased with no statistical significance.

Discussion

Although the use of disease modifying therapies has been able to modify the autoimmune or inflammatory components of MS, it is unclear whether these agents can prevent the progression of the disease [17]. Hence, in this study we attempt to investigate whether the use of MSC as a therapeutic option can have an effect on the disease progression. EAE is the most widely accepted model of MS and review of previous studies advocates that in many instances disease amelioration and prevention is possible if a treatment is initiated near the onset of EAE symp-

toms. In a previous study, EAE symptoms appeared 8 to 12 days after immunization with MOG in C57BL/6 mouse [18]. Adipose tissue derived MSCs were given intravenously on day 12 and day 14. Significant difference in the clinical scores between untreated and MSC-treated EAE groups of mice was found only on the 20th day and onwards. In a separate study, MSCs were injected on day 18 and day 30 after immunization with MOG in C57BL/6 mouse [19]. Early improvement in the clinical scores was observed when MSCs were administered on day 18, but there was no effect when MSCs were administered on day 30. A significant decrease in Th17 cells and an increase in CD4⁺CD25⁺foxp3⁺ T-cells were observed in the lymph node of only those EAE mice that received MSCs on day 18. In the present study, the EAE mice reached a mean clinical score of 1.88, on 10th day after immunization with MOG. MSCs were administered intravenously on 11th day, and significant improvement in the clinical score was observed day 16 onwards.

A number of studies using the EAE model, have used various behavioral tests to assess the motor impairment. In a study evaluating pregabalin treatment on EAE model, contact area of each hind limb footprint was used in walking track test for motor evaluation [20]. In another study, where optimized dosage of MOG immunization was used in Lewis rats, moderate impairment of hind limb locomotor function was detected in grid walk test at day 3, and the animals recovered by day 14 [21]. In our study, we used the stride length of foot print analysis to evaluate the locomotor function in EAE mice following MSC treatment, which has not been previously reported.

In the sham-treated control mice group, no significant change was observed in the mean value of the hindlimb stride length in the post-experiment days compared to day 0 (pre-experiment observation). In the PBS-treated EAE mice group, significant reduction ($P < 0.05$) in the mean values of the left (day 10 onwards) and right hind limb stride length (day 15 onwards) was observed. Following intravenous injection of MSC on day 11, significant elevation ($P < 0.05$) in the mean values of the left and right hind limb stride length was observed in the MSC-treated EAE mice group on day 15 and day 20, compared to day 10. Zappia *et al.* in a study on transplantation of MSCs in the

EAE model of multiple sclerosis, proposed that the majority of the transplanted MSCs migrated to the secondary lymphoid organs and clinical improvement appeared to be mediated by the inhibition of peripheral encephalitogenic T-cells [22]. There was little evidence that the transplanted MSCs differentiate into neurons. Improvement in the clinical motor function requires replenishment of damaged myelin. Increase in the number of oligodendrocytes, glial cells responsible for myelination in the spinal cord, was observed in the histological analysis of MSC-treated EAE animals [23, 24].

The present study found evidence of demyelination in the lateral funiculi of LFB-stained lumbar spinal cord sections PBS-treated EAE group of mice. In MSC-treated EAE group of mice, many normal looking axons were observed in the anterior and lateral funiculi of lumbar spinal cord sections under H&E staining. A study evaluating the effect of intravenous adipose tissue derived MSCs in a chronic EAE model, found 51% decrease in the demyelinated areas and 42% decrease in the axonal loss in the white matter of lumbar spinal cord in MSC-treated EAE mice compared to control vehicle-treated EAE mice [25].

IL-17 plays an important role in regulating the adaptive and innate immunity, as well as in host defense and the pathogenesis of certain autoimmune diseases. IL-17 receptor mRNA has been found to be expressed in the lungs, kidney, liver, spleen and various myeloid cells [26]. Th17 cells, named after their ability to secrete IL-17, have been proven to play an essential role in the pathogenesis of early phase of autoimmune CNS inflammation such as MS [27]. The present study used a single dose of MSC treatment, administered intravenously, at the peak of the EAE symptom development (day 11 after immunization with MOG). When CD4⁺T cells differentiated into Th17 cells, were co-cultured with MSCs, IL-17 secreting cells were suppressed. The maximum suppression of IL-17 secreting cells was achieved when MSCs were added at the beginning or day zero of the differentiation process [19]. Lack of significant increase of IL-17 levels in the spleen of the different mice of the MSC treated EAE group was possibly due to different stages of the TH17 differentiation process among the members of the group. Therapeutic effect of MSC treatment in the early stage of EAE model

Effect of MSC on EAE model in mouse

was found to be associated with both significant decrease of Th17 cells and increase of CD4⁺CD25⁺Foxp3⁺ T regulatory cells [17].

Conclusion

The present study was able to produce a limited level of motor function loss restricted to the hindlimb of C57BL/6 mouse model of EAE by immunization with MOG. MSCs isolated from the culture of syngeneic mouse compact bone and given intravenously to the EAE mice, were able to increase the motor functions of both hindlimbs. This was evidenced by significant increase in the stride length and improvement in the clinical score in the mice receiving the MSC treatment. Qualitative histological observation of the lumbar spinal cord provided evidence of improvement in the morphology of the myelinated white matter following MSC treatment. Changes in the IL-17 levels in the spleen following MSC treatment could not be established.

Acknowledgements

This work was supported by research grant from the Centre for Research and Development of Taylor's University, Malaysia granted to NKM. The authors acknowledge the support from the Brain Research Institute of Monash University Sunway Campus, Malaysia for use of the animal facility for the maintenance of the animals.

Disclosure of conflict of interest

None.

Address correspondence to: Nilesh Kumar Mitra, School of Medicine, Taylor's University, No. 1 Jalan Taylor's, Subang Jaya, Selangor, Malaysia. Tel: 603-56295495; Fax: 603-56295455; E-mail: Nilesh-Kumar.Mitra@taylors.edu.my

References

- [1] Kamm C, Zettl UK. Autoimmune disorders affecting both the central and peripheral nervous system. *Autoimmun Rev* 2012; 11: 196-202.
- [2] Javed A, Reder AT. Therapeutic role of beta-interferons in multiple sclerosis. *Pharmacol Ther* 2006; 110: 35-56.
- [3] Hemmer B, Archelos JJ, Hartung HP. New concepts in the immunopathogenesis of multiple sclerosis. *Nat Rev* 2002; 3: 291-301.

- [4] Gold R, Linington C, Lassmann H. Understanding pathogenesis and therapy of multiple sclerosis via animal models: 70 years of merits and culprits in experimental autoimmune encephalomyelitis research. *Brain* 2006; 129: 1953-1971.
- [5] Swanborg RH. Experimental autoimmune encephalomyelitis in rodents as a model for human demyelinating disease. *Clin Immunol Immunopathol* 1995; 77: 4-13.
- [6] Dyer CA. Novel oligodendrocyte transmembrane signaling systems. *Mol Neurobiol* 1993; 7: 1-22.
- [7] Kerlero de Rosbo N, Hoffman M, Mendel I, Yust I, Kaye J, Bakimer R, Flechter S, Abramsky O, Milo R, Karni A, Ben-Nun A. Predominance of the autoimmune response to myelin oligodendrocyte glycoprotein (MOG) in multiple sclerosis: reactivity to the extracellular domain of MOG is directed against three main regions. *Eur J Immunol* 1997; 27: 3059-3069.
- [8] Hartung HP, Kieseier BC, Hemmer B. Purely systemically active anti-inflammatory treatments are adequate to control multiple sclerosis. *J Neurol* 2005; 252: v30-v37.
- [9] Bruck W. The pathology of multiple sclerosis is the result of focal inflammatory demyelination with axonal damage. *J Neurol* 2005; 252: v3-v9.
- [10] Bianco P, Robey PG, Simmons PJ. Mesenchymal stem cells: revisiting history, concepts, and assays. *Cell Stem Cell* 2008; 2: 313-319.
- [11] Prockop DJ, Gregory CA, Spees JL. One strategy for cell and gene therapy: harnessing the power of adult stem cells to repair tissues. *Proc Natl Acad Sci U S A* 2003; 100: 11917-11923.
- [12] van Velthoven CT, Kavelaars A, van Bel F, Heijnen CJ. Regeneration of the ischemic brain by engineered stem cells: fuelling endogenous repair processes. *Brain Res Rev* 2009; 61: 1-13.
- [13] Bartholomew A, Sturgeon C, Siatskas M, Ferrer K, McIntosh K, Patil S, Hardy W, Devine S, Ucker D, Deans R, Moseley A, Hoffman R. Mesenchymal stem cells suppress lymphocyte proliferation in vitro and prolong skin graft survival in vivo. *Exp Hematol* 2002; 30: 42-48.
- [14] Di Nicola M, Carlo-Stella C, Magni M, Milanese M, Longoni PD, Matteucci P, Grisanti S, Gianni AM. Human bone marrow stromal cells suppress T-lymphocyte proliferation induced by cellular or nonspecific mitogenic stimuli. *Blood* 2002; 99: 3838-3843.
- [15] Mitra NK, Tan CY, Bindal U, Chua CLL, Wong EH, Parhar IS, Soga T. Investigating cell surface markers and differentiation potential of compact bone-derived mesenchymal stem cells. *Int J Stem Cell Res Transplant* 2015; 3: 91-95.
- [16] Anderson P, Carrillo-Gálvez AB, García-Pérez A, Cobo M, Martín F. CD105 (endoglin)-negative

Effect of MSC on EAE model in mouse

- murine mesenchymal stromal cells define a new multipotent subpopulation with distinct differentiation and immunomodulatory capacities. *PLoS One* 2013; 8: e76979.
- [17] Freedman MS. Long term follow-up of clinical trials of multiple sclerosis therapies. *Neurology* 2011; 76: S26-S34.
- [18] Yousefi F, Ebtekar M, Soleimani M, Soudi S, Hashemi SM. Comparison of in vivo immunomodulatory effects of intravenous and intraperitoneal administration of adipose tissue mesenchymal stem cells in experimental autoimmune encephalomyelitis (EAE). *Int Immunopharmacol* 2013; 17: 608-616.
- [19] Luz-Crawford P, Kurte M, Bravo-Alegría J, Contreras R, Nova-Lamperti E, Tejedor G, Noël D, Jorgensen C, Figueroa F, Djouad F, Carrión F. Mesenchymal stem cells generate a CD4⁺CD25⁺Foxp3⁺ regulatory T cell population during the differentiation process of Th1 and Th17 cells. *Stem Cell Res Ther* 2013; 4: 65.
- [20] Silva GA, Pradella F, Moraes A, Farias A, dos Santos LM, de Oliveira AL. Impact of pregabalin treatment on synaptic plasticity and glial reactivity during the course of experimental autoimmune encephalomyelitis. *Brain Behav* 2014; 4: 925-935.
- [21] Kerschensteiner M, Stadelmann C, Buddeberg BS, Merkler D, Bareyre FM, Anthony DC, Linington C, Brück W, Schwab ME. Targeting experimental autoimmune encephalomyelitis lesions to a predetermined axonal tract system allows for refined behavioral testing in an animal model of multiple sclerosis. *Am J Pathol* 2004; 164: 1455-1469.
- [22] Zappia E, Casazza S, Pedemonte E, Benvenuto F, Bonanni I, Gerdoni E, Giunti D, Ceravolo A, Cazzanti F, Frassoni F, Mancardi G, Uccelli A. Mesenchymal stem cells ameliorate experimental autoimmune encephalomyelitis inducing T-cell anergy. *Blood* 2005; 106: 1755-1756.
- [23] Rasmusson I, Ringdén O, Sundberg B, Le Blanc K. Mesenchymal stem cells inhibit the formation of cytotoxic T lymphocytes, but not activated cytotoxic T lymphocytes or natural killer cells. *Transplantation* 2003; 76: 1208-1213.
- [24] Bai L, Lennon DP, Eaton V, Maier K, Caplan AI, Miller SD, Miller RH. Human bone marrow-derived mesenchymal stem cells induce Th2-polarized immune response and promote endogenous repair in animal models of multiple sclerosis. *Glia* 2009; 57: 1192-1203.
- [25] Bifari F, Galiè M, Turano E, Budui S, Sbarbati A, Krampera M, Bonetti B. Adipose-derived mesenchymal stem cells ameliorate chronic experimental autoimmune encephalomyelitis. *Stem Cells* 2009; 27: 2624-2635.
- [26] Kolls JK, Lindén A. Interleukin-17 family members and inflammation. *Immunity* 2004; 21: 467-476.
- [27] Rostami A, Ciric B. Role of Th17 cells in the pathogenesis of CNS inflammatory demyelination. *J Neurol Sci* 2013; 333: 76-87.